to the quality as well as the quantity of mtDNA or RNA sequences. In that way, the nuclear genome could "sense" the amount or kind of mtDNA in the cell.

Whether different ρ^- mtDNA's, such as those containing the genes for the large or small rRNA's, both of which can be transcribed and correctly processed in petites, can affect expression of genes encoding mitochondrial ribosomal proteins or other nuclear-encoded mitochondrial translation factors remains to be determined. Many similar questions can also be asked concerning other sequences along the yeast mitochondrial genome.

REFERENCES AND NOTES

1. G. Schatz and T. L. Mason, *Annu. Rev. Biochem.* **43**, 51 (1974); B. Dujon, in *The Molecular Biology of the Yeast Saccharomyces: Life Cycle and Inheritance*, J. Strathern, E. Jones, J. Broach, Eds. (Cold Spring Harbor Laboratory, Cold Spring Harbor, NY, 1981), p. 505.
2. L. Guarente and T. Mason, *Cell* **32**, 1279 (1983).
3. E. Szekely and D. L. Montgomery, *Mol. Cell. Biol.* **4**, 939 (1984).
4. R. M. Wright, C. Ko, M. G. Cumsky, R. O. Poyton, *J. Biol. Chem.* **259**, 15401 (1984).
5. W. Dowhan, C. R. Bibus, G. Schatz, *EMBO J.* **4**, 179 (1985).
6. L. Guarente, B. Lalonde, P. Gifford, E. Alani, *Cell* **36**, 503 (1984).
7. H. R. Mahler *et al.*, in *Mitochondria 1977: Genetics and Biogenesis of Mitochondria*, W. Bandlow, R. J. Schweyen, K. Wolf, F. Kaudewitz, Eds. (de Gruyter, New York, 1977), p. 345.
8. H. Blanc and B. Dujon, *Proc. Natl. Acad. Sci. U.S.A.* **77**, 3942 (1980); G. Bernardi *et al.*, in *The Organization and Expression of Mitochondrial Genomes*, A. M. Kroon and C. Saccone, Eds. (Elsevier/North-Holland, Amsterdam, 1980), p. 21; M. de Zamaroczy *et al.*, *Nature (London)* **292**, 75 (1981).
9. T. Maniatis, E. F. Fritsch, J. Sambrook, *Molecular Cloning: A Laboratory Manual* (Cold Spring Harbor Laboratory, Cold Spring Harbor, NY, 1982), p. 241.
10. D. Shortle, J. E. Haber, D. Botstein, *Science* **217**, 371 (1982); P. Novick and D. Botstein *Cell* **40**, 405 (1985).
11. K. G. Skryabin *et al.*, *Nucleic Acids Res.* **12**, 2955 (1984).
12. V. Parikh, unpublished observations.
13. R. A. Kramer, P. Phillippsen, R. W. Davis, *J. Mol. Biol.* **123**, 405 (1978).
14. M. E. Swanson and M. J. Holland, *J. Biol. Chem.* **258**, 3242 (1983).
15. H. Zalkin *et al.*, *ibid.* **259**, 3985 (1984).
16. G. P. Thill *et al.*, *Mol. Cell. Biol.* **3**, 570 (1983).
17. J. L. Hartley and J. E. Donelson, *Nature (London)* **286**, 860 (1980).
18. J. R. Broach, in *The Molecular Biology of the Yeast Saccharomyces: Life Cycle and Inheritance*, J. Strathern, E. Jones, J. Broach, Eds. (Cold Spring Harbor Laboratory, Cold Spring Harbor, NY, 1981), p. 445; M. Jayaram, Y.-Y. Li, J. R. Broach, *Cell* **34**, 95 (1984).
19. J. R. Cameron, R. Philippsen, R. W. Davis, *Nucleic Acids Res.* **4**, 1429 (1977).
20. J. R. Broach, J. F. Atkins, C. McGill, L. Chow, *Cell* **16**, 827 (1979).
21. R. S. Zitomer, D. L. Montgomery, D. L. Nichols, B. D. Hall, *Proc. Natl. Acad. Sci. U.S.A.* **76**, 3627 (1979).
22. I. H. Evans and D. Wilkie, in *The Genetic Function of Mitochondrial DNA*, C. Saccone and A. M. Kroon, Eds. (Elsevier/North-Holland, Amsterdam, 1976), p. 209.
23. N. Gunge and C. Yamane, *J. Bacteriol.* **159**, 533 (1984).
24. K. F. Lindahl and K. Bürki, *Proc. Natl. Acad. Sci. U.S.A.* **79**, 5362 (1982); K. F. Lindahl, B. Hausmann, V. M. Chapman, **6**, *Nature (London)* **306**, 383 (1983); K. F. Lindahl and B. Hausmann, *Genetics* 103, 483 (1983).
25. R. Smith III *et al.*, *Nature (London)* **306**, 599 (1983).
26. S. R. Ellis, M. J. Morales, J.-M. Li, A. K. Hopper, N. C. Martin, *J. Biol. Chem.* **261**, 9703 (1986).
27. G. Natsoulis, F. Hilger, G. R. Fink, *Cell* **46**, 235 (1986).
28. J. M. Chirgwin, A. E. Przybyla, R. J. MacDonald, W. J. Rutter, *Biochemistry* **18**, 5294 (1979).
29. K. Nasmyth, *Nature (London)* **302**, 670 (1983).
30. H. Aviv and P. Leder, *Proc. Natl. Acad. Sci. U.S.A.* **69**, 1408 (1972).
31. R. Ng and J. Abelson, *ibid.* 77, 3912 (1980).
32. R. W. Davis *et al.*, *Methods Enzymol.* **65**, 404 (1980).
33. F. Sanger, S. Nicklen, A. R. Coulson, *Proc. Natl. Acad. Sci. U.S.A.* **74**, 5463 (1977).
34. M. Takeda *et al.*, *J. Biol. Chem.* **260**, 15458 (1985).

35. Supported by grants from the NIH and the Robert A. Welch Foundation. We thank Jim Broach, Michael Douglas, Robert Poyton, and Fred Sherman for providing probes; Kirsten Fischer-Lindahl for reading of the manuscript; and Marie Rotondi for help in preparation of the manuscript.

8 August 1986; accepted 16 November 1986

Human Neuroelectric Patterns Predict Performance Accuracy

ALAN S. GEVINS, NELSON H. MORGAN, STEVEN L. BRESSLER, BRIAN A. CUTILLO, ROSEANN M. WHITE, JUDY ILLES, DOUGLAS S. GREER, JOSEPH C. DOYLE, GERALD M. ZEITLIN

In seven right-handed adults, the brain electrical patterns before accurate performance differed from the patterns before inaccurate performance. Activity overlying the left frontal cortex and the motor and parietal cortices contralateral to the performing hand preceded accurate left- or right-hand performance. Additional strong activity overlying midline motor and premotor cortices preceded left-hand performance. These measurements suggest that brief, spatially distributed neural activity patterns, or "preparatory sets," in distinct cognitive, somesthetic-motor, and integrative motor areas of the human brain may be essential precursors of accurate visuomotor performance.

PREPARATORY SET FOR HUMAN VISUOMOTOR performance, defined as a state of readiness to receive a stimulus or make a response (*1*), has been studied by a variety of disciplines. Temporal properties of preparatory sets have been measured in information-processing studies, but such studies have not focused on the underlying neural systems (*2*). Spatial properties of preparatory sets measured in cerebral blood flow studies have revealed increased metabolic activity for sensory-specific focus of attention in superior prefrontal, midfrontal, and anterior parietal cortices (*3*). These studies have been limited, however, by the temporal resolution (1 minute or longer) of blood flow measurement techniques. Clinical neuropsychological studies have demonstrated that behaviors requiring preparatory sets (*4*) rely on intact lateral frontal regions (*5*), but variability in size and location of lesions has limited the spatial specificity of such studies in localizing normal function. And although scalp-recorded brain electrical and magnetic recordings provide both spatial and temporal information on neural activity underlying preparatory sets, studies of the contingent negative variation (CNV), an event-related brain potential component thought to be related to preparatory set, have often yielded controversial or ambiguous results (*6*).

Recording from 26 electrodes and using several signal-enhancing procedures, we measured the rapidly changing spatial patterns of mass neuroelectric activity associated with preparation and execution of precise right- and left-hand finger pressures in response to visual numeric stimuli. We found differences occurring during the prestimulus period between patterns associated with subsequently accurate and inaccurate performance. These group differences allowed discrimination of subsequent performance accuracy for both hands of individual subjects. Thus, a spatially specific, multicomponent neural preparatory set, composed of an invariant left frontal component and hand-specific central and parietal components, may be essential for accurate performance of certain types of difficult visuomotor tasks.

Seven healthy, right-handed male adults were recruited from the community and paid for their participation. They were required to exert rapid, precisely graded pressures (forces from 0.1 to 0.9 kg) followed by immediate release, with right- and left-hand index fingers in response to visual numeric stimuli (numbers 1 to 9). The stimulus was presented randomly on successive trials 1 second after a cue (the letter *V* lasting 0.3 second) that was slanted at a 30° angle to the right or left to indicate the required response hand (*7*). In "respond" trials, the

EEG Systems Laboratory, 1855 Folsom Street, San Francisco, CA 94103.

stimulus was slanted in the same direction as the cue, and the subject was to respond quickly with finger pressure of the indicated hand, with a force corresponding to the stimulus number on a linear scale from 1 to 9. In a random 20% of the trials, the stimulus was slanted opposite to the cue and the subject was to make no response. These miscued "catch" trials ensured that subjects attended to the cues and stimuli. To help subjects calibrate their responses, the pressure produced was displayed 1 second after completion of each response (*8*).

Brain potentials from 26 scalp electrodes (*9*), vertical and horizontal eye movement potentials, and flexor digitori muscle potentials were recorded onto magnetic tape at 128 Hz from 0.75 second before the cue to 1 second after feedback (*10*). The Laplacian operator, a spatial pattern enhancement technique, was applied to the brain potentials at every time point to reduce the blur distortion that results as potentials are transmitted from the brain to the scalp (*11*). Two independent raters edited the data for artifacts by visual inspection of brain, eye movement, and muscle potential polygraph channels. Trials with artifacts due to eye movement, head or electrode movement, or scalp muscle contamination were eliminated, as were trials with slow, bimodal, or delayed responses, or with flexor digitorum activity between the cue and the stimulus.

The remaining trials (60%) were then sorted for response accuracy, and the two sets of trials were balanced according to a number of criteria to avoid confounding performance variations due to transitory and longer lasting changes in arousal and learning with inaccuracy per se. Accurate and inaccurate data sets consisted of trials in which the error (deviation from required pressure) for each subject was, respectively, less and greater than his mean error over all remaining trials (*12*). Mean reaction time, averaged across all subjects, was consistent among hand and accuracy conditions (610 to 618 msec).

To quantitate the electrical activity of the brain, we measured the covariance (similarity of wave shape) between different pairs of electrodes over brief segments (187 or 375 msec) of event-related (cue, stimulus, response, feedback) waveforms averaged from the seven subjects (*13–15*). Covariances between each of the 120 combinations of the 16 Laplacian-transformed channels were computed from enhanced (*16*) and filtered average waveforms. We determined the covariance for each electrode pair by computing the cross-covariance function between their waveform segments, with the lag time for one channel with respect to the other varying from 0 to 125 msec. The value of covariance was the maximum absolute value of that function. For the wave at the peak of the response, covariances were analyzed to determine whether they were significantly different from noise values (*17, 18*); we could then compare the levels of significance of each electrode pair under different experimental conditions.

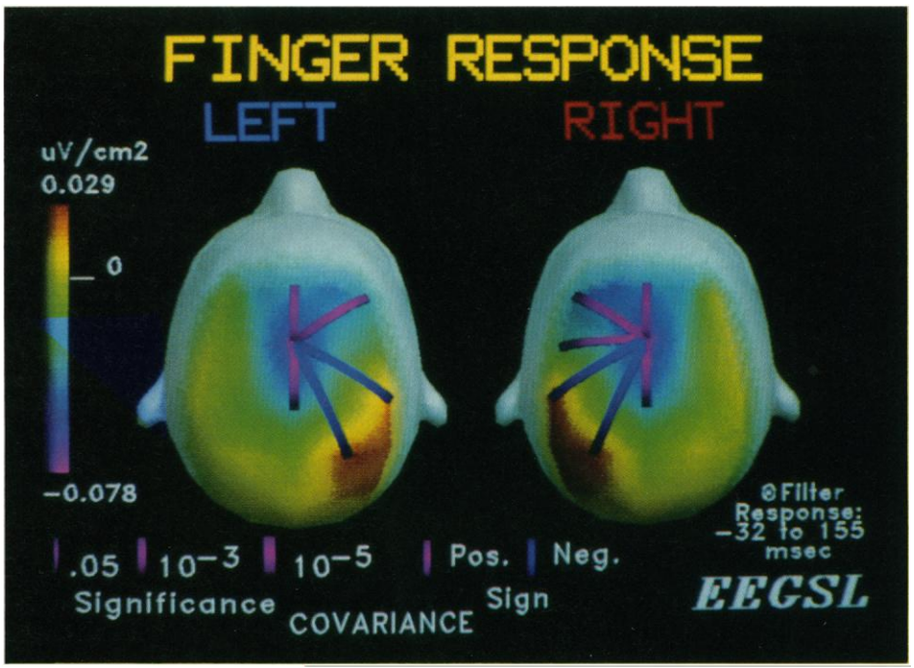

Fig. 1. Most significant, between-channel covariance patterns (colored lines), looking down at the top of the head, from the wave at the peak of the response superimposed on colored maps of that wave's amplitude. The motor-related wave was measured during a 187-msec interval centered on the peak of left-hand and right-hand index finger pressures from seven right-handed men (*19*). The thickness of a covariance line is proportional to the negative logarithm of its significance (from 0.05 to 0.00005) (*17*). A violet line indicates a positive covariance (motor-related waves with the same polarity), and a blue line indicates a negative covariance (motor-related waves with opposite polarities). The color scale at the left, representing wave amplitude, covers the range from the minimum to maximum values of the two maps. All covariances refer to the site overlying supplementary and premotor cortices. There is a strong lateralization of frontal, central, and antero-parietal covariances over the hemisphere contralateral to the responding hand, a result consistent with the lateralization of the amplitude maps.

To validate the analysis in a known case, this procedure was applied to waveforms time-registered to the onset of the finger pressure response. The most significant left- and right-hand covariances occurred between electrodes overlying cortical regions involved in motor execution (Fig. 1) (*19*). These patterns of covariance presented much more spatially discrete information than their corresponding amplitude maps (*20*). In the 187-msec interval centered on the peak of the response (62 msec after response onset), right- and left-hand covariance patterns were nearly mirror images. In both patterns all covariances involved the midline antero-central site overlying the premotor and supplementary motor cortices. Covariances between this site and the left frontal, antero-central, central, and antero-parietal sites for right-hand responses, and between corresponding right-hemisphere sites (except right antero-central) for the left hand, were all consistent with known motor-related cortical areas.

The procedure was then applied to the cue-to-stimulus period to study preparatory sets (*21*). Statistical comparison of the CNV amplitudes (Fig. 2) during an interval 500 to 875 msec after the cue did not reveal significant differences between accurate and inaccurate conditions (*22*). During this same period, however, well-defined between-channel covariance patterns related to subsequent accuracy were discovered. They first appeared in the interval centered 500 msec after the cue and became well differentiated between accurate and inaccurate conditions in the 500- to 875-msec interval (centered 313 msec before stimulus onset) spanning the late component of the CNV. The lack of muscle potential and eye movement signals in these intervals confirmed that these patterns were neural in origin (Fig. 3).

Covariance patterns during the period between the cue and the stimulus (Fig. 4) were distinct from those related to overt finger responses. During the interval from 500 to 875 msec after the cue onset, covariance patterns associated with subsequently

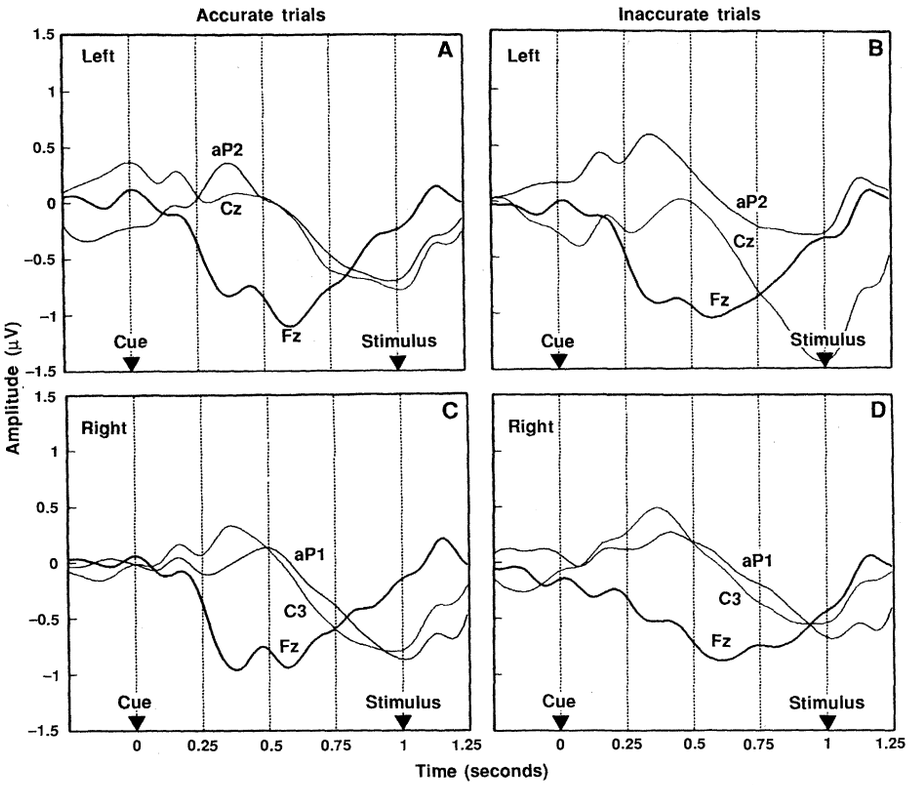

Fig. 2. Amplitudes of the CNV computed during the cue-to-stimulus period. Amplitudes between low-pass filtered (below 3 Hz), event-related Laplacian waveforms, averaged from seven subjects, are not significantly different for the comparison of (**A**) left-accurate (252 to 274 trials) with (**B**) left-inaccurate (254 to 284 trials) conditions, or (**C**) right-accurate (291 to 309 trials) with (**D**) right-inaccurate (282 to 304 trials) conditions.

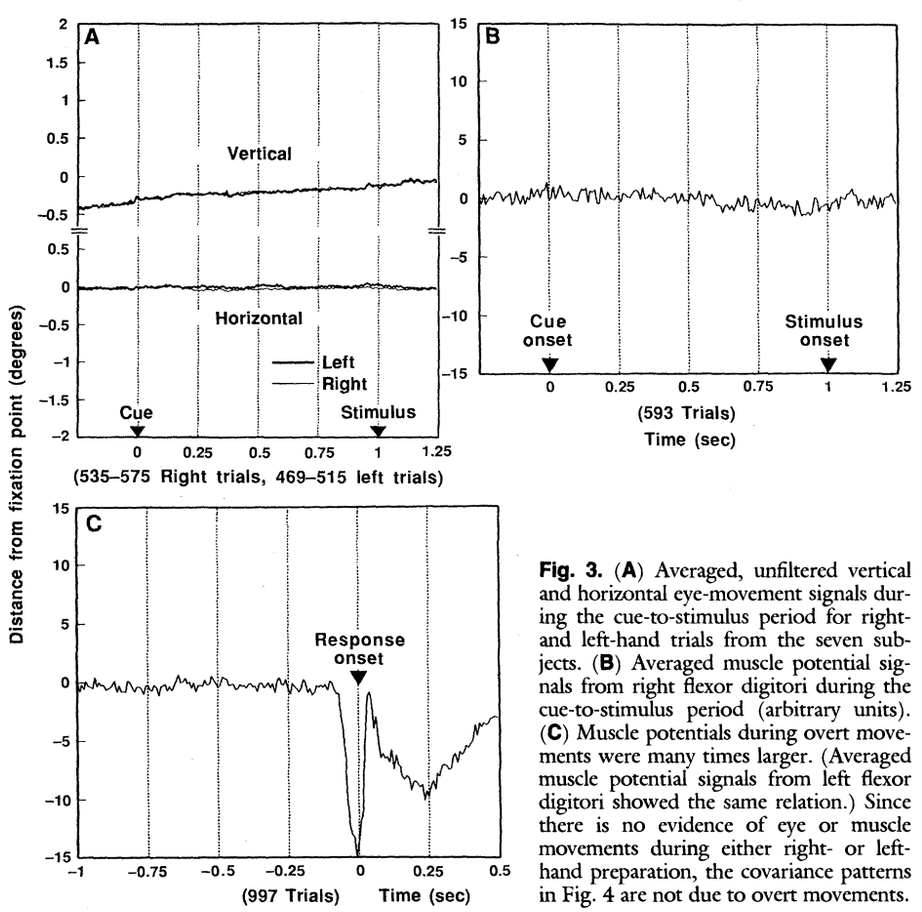

Fig. 3. (**A**) Averaged, unfiltered vertical and horizontal eye-movement signals during the cue-to-stimulus period for right- and left-hand trials from the seven subjects. (**B**) Averaged muscle potential signals from right flexor digitori during the cue-to-stimulus period (arbitrary units). (**C**) Muscle potentials during overt movements were many times larger. (Averaged muscle potential signals from left flexor digitori showed the same relation.) Since there is no evidence of eye or muscle movements during either right- or left-hand preparation, the covariance patterns in Fig. 4 are not due to overt movements.

accurate right-hand performance involved predominantly left hemisphere sites, particularly left frontal, central, parietal, and antero-parietal sites (*23*). All 24 significant covariances involved sites on the left side, and 18 (75%) of these were exclusively on the left side. The covariance pattern preceding subsequently accurate left-hand performance for this interval involved predominantly right-hemisphere sites. Of 18 significant covariances in this pattern, 13 (72%) involved right hemispheric sites. The right-sided central, parietal, and antero-parietal sites were most prominent, compared with corresponding prominent contralateral sites for the right-hand accurate pattern. The left frontal site was prominent before both left- and right-hand performance. The midline central and antero-central sites were prominent in the left-hand pattern but were not among the most prominent in the right-hand pattern.

Only two significant covariances were related to subsequently inaccurate right-hand performance in this interval, namely, left parietal with left frontal and antero-parietal with left frontal. In contrast, the subsequently inaccurate covariance pattern for the left hand was more bilateral and complex than the subsequently accurate pattern. The patterns for the two accuracy conditions differed both in scale and pattern for the left hand, but only in scale for the right hand (*24*). Unlike the between-channel covariance patterns, the CNV amplitude maps were highly similar for both accuracy conditions and hands and were not useful in determining what areas would covary.

Through the use of statistical pattern classification procedures, covariances shown in Fig. 4 were considered possible variables to distinguish subsequent performance accuracy. The trials of each of the seven subjects were classified by equations developed on the trials of the other six subjects (*25*). The overall discrimination of subsequently accurate from subsequently inaccurate trials was 59% ($P < 0.01$) for right-hand and 57% ($P < 0.01$) for left-hand performance. Discrimination of subsequent right-hand performance accuracy was above 57% for six subjects but was 50% for the seventh. For left-hand performance, discrimination for three subjects ranged from 56% to 67%, and was 53% or below for four subjects (who had fewer trials overall). Average classification of each fifth of the trials from the four subjects with lowest left-hand discrimination, calculated from equations developed from the other four-fifths, was 61% ($P < 0.001$). This suggests that the four subjects had similar covariance patterns before left-hand performance, which differed from those of the other three subjects. The

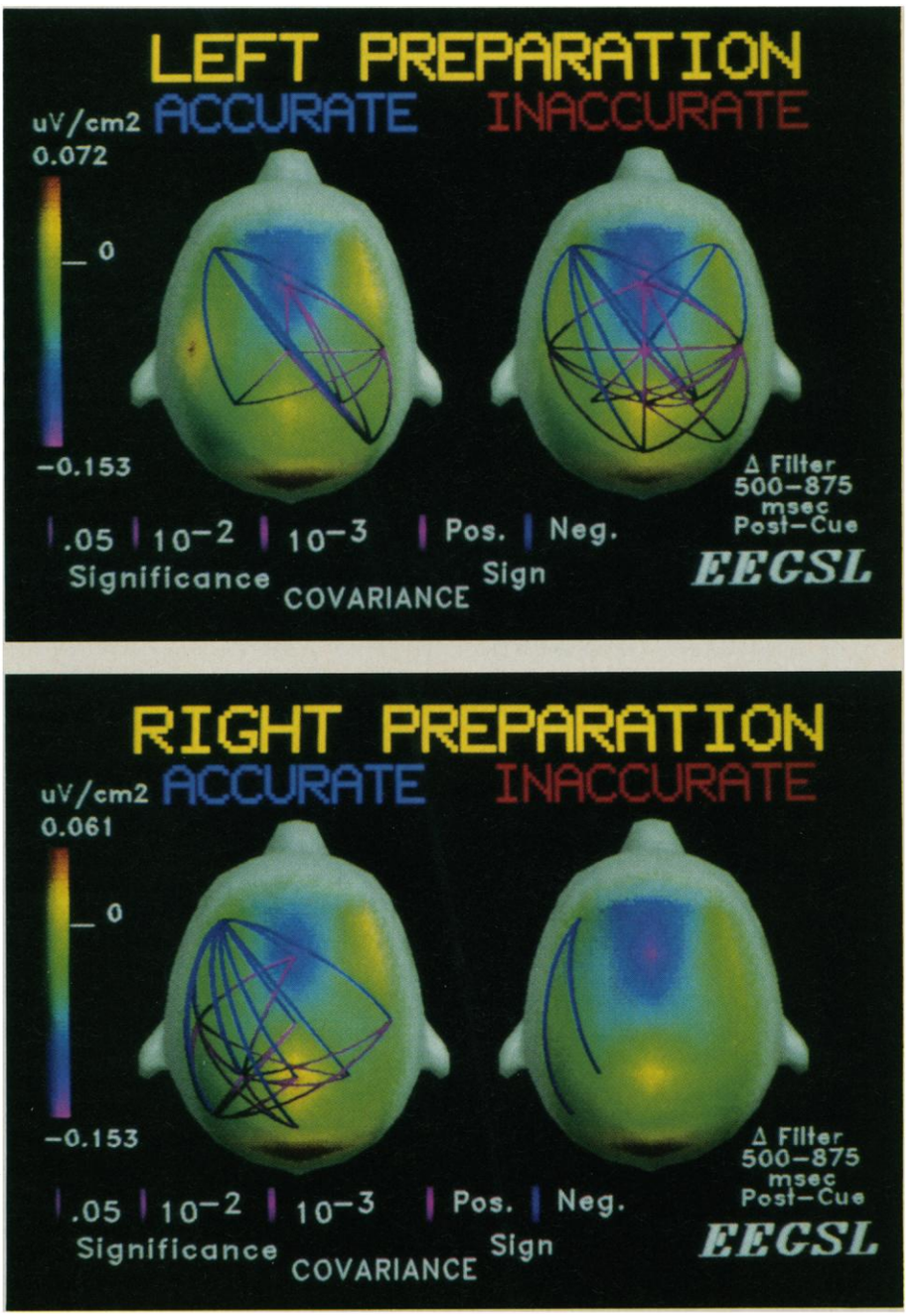

Fig. 4. View of the significant ($P < 0.05$) between-channel CNV covariance patterns, looking down at the top of the head, superimposed on maps of CNV amplitude. Measurements are from an interval 500 to 875 msec after the cue for subsequently accurate and inaccurate left-hand (**top**) and right-hand (**bottom**) visuomotor task performance by seven right-handed men. The thickness of a covariance line is proportional to the negative logarithm of its significance (from 0.05 to 0.001). A violet line indicates the covariance is positive, while a blue line is negative. Covariances involving left frontal and appropriately contralateral central and parietal electrode sites are prominent in patterns for subsequently accurate performance of both hands. The magnitude and number of covariances are greater before subsequently inaccurate left-hand performance by these right-handed subjects and are more widely distributed than the left-hand accurate pattern. For the right hand, fewer and weaker covariances characterize subsequently inaccurate performance. The amplitude maps are similar for the four conditions and do not indicate any of the specific differences evident in the covariance patterns.

greater uniformity for right- over left-hand discrimination suggests that there are similar covariance patterns among the strongly right-handed subjects preceding accurate and inaccurate right-hand performance, and a divergence of patterns preceding left-hand performance. Although there were differences in discriminative power between individuals, overall the group preparation patterns were effective in deciding an individual's subsequent performance accuracy. For the one subject with the most trials, an average classification of 68% ($P < 0.001$) for subsequent right-hand and 62% ($P < 0.01$) for subsequent left-hand performance was achieved by testing a separate equation on each fifth of his trials, formed from the other four-fifths.

Although the origin of these event-related, between-channel covariance patterns of preparatory sets is unknown (*26*), our results suggest that preparation for accurate performance in a visuomotor task involves several brain components (*27*): a cognitive component manifested by invariant activity at the left frontal covariance site, a hand-specific somesthetic-motor component manifested by the contralateral central and parietal sites, and an integrative motor component manifested by activity at the midline central and antero-central sites. The last component was strong in the pattern preceding accurate left-hand performance and weaker in the pattern preceding accurate right-hand performance. For both hands, preparatory covariance patterns were different from those accompanying actual response execution. Covariance patterns preceding inaccurate performance by each hand differed markedly. The relative lack of significant covariances preceding inaccurate right-hand performance may be interpreted as evidence for a weakened preparatory set. By contrast, the complex, anatomically diffuse but strong patterns in the left-hand condition suggest that inaccurate performance by the nondominant hand of strongly right-handed subjects may result from erroneous, possibly confounded, preparatory sets.

Our evidence for distributed, coordinated preparatory components of human visuomotor performance is consistent with earlier studies of this behavior. The involvement of the left frontal site is consistent with evidence that preparatory sets in humans are synthesized and integrated in left dorsolateral prefrontal cortices (*4, 5*). The finding of an appropriately lateralized parieto-central somesthetic-motor component is consistent with data that show neuronal firing patterns before motor responses in the motor cortex of nonhuman primates and localized potentials in the somesthetic cortex of humans at the same time (*1, 28*). Finally, a midline antero-central integrative motor component is consistent with known involvement of premotor and supplementary motor regions in initiating existing motor schemes and establishing new ones (*3, 29*).

Our results demonstrate that the human brain, unlike a fixed-program computer, dynamically "programs" its distributed, specialized subsystems in anticipation of the

need to process certain types of information and take certain types of action. When these preparatory sets are incomplete or incorrect, subsequent performance is likely to be inaccurate.

REFERENCES AND NOTES

1. E. V. Evarts, Y. Shinoda, S. P. Wise, *Neurophysiological Approaches to Higher Brain Functions* (Wiley, New York, 1984).
2. M. Posner, *Chronometric Explorations of the Mind* (Erlbaum, Hillsdale, NJ, 1978).
3. P. E. Roland, *J. Neurophysiol.* **48**, 744 (1982); *Human Neurobiol.* **4**, 155 (1985); in *Brain Imaging and Brain Function*, L. Sokoloff, Ed. (Raven, New York, 1985), pp. 87–104.
4. D. T. Stuss and D. F. Benson, *The Frontal Lobes* (Raven, New York, 1986).
5. A. R. Luria, *Higher Cortical Functions in Man* (Basic Books, New York, 1966); H. L. Teuber, in *The Frontal Granular Cortex and Behavior*, J. M. Warren and K. Akert, Eds. (McGraw-Hill, New York, 1964); B. Milner and M. Petrides, *Trends Neurosci.* 7, 43 (1984); P. S. Goldman-Rakic, *ibid.*, p. 419.
6. J. J. Tecce, *Psychol. Bull.* 77, 73 (1972); J. W. Rohrbaugh, K. Syndulko, T. F. Sanquist, D. B. Lindsley, *Science* **208**, 1165 (1980); A. W. K. Gaillard and W. Ritter, Eds., *Advances in Psychology*, vol. 10, *Tutorials in Event-Related Potential Research* (Elsevier, Amsterdam, 1983); A. Gevins and B. Cutillo, in *Application of Computer Analysis to EEG. Handbook of Electroencephalography and Clinical Neurophysiology*, F. Lopes da Silva, S. Van Leeuwen, A. Remond, Eds. (Elsevier, Amsterdam, 1987), vol. 2.
7. The cue, stimulus, and feedback were presented on a Videographics-II cathode ray tube monitor located 70 cm from the subject and were of equal duration and visual angle (under 1°).
8. Feedback indicating exact response pressure to one-tenth of a stimulus unit was presented as a two-digit number 1 second after the peak of response. The feedback number was underlined to indicate a "win" when the response error was less than the recent performance level, which was updated on-line after each trial as the average error from the preceding five trials for each hand separately. This criterion made it harder for the subject to win the monetary bonus (5 cents) paid for "win" trials as performance improved. This technique and rest breaks minimized possible systematic changes in arousal. Monetary penalties (10 cents) were deducted only for responding to miscued "catch" trials. Each subject performed between 900 and 1000 trials over a period of 5 to 6 hours, with frequent rest breaks. Subjects practiced the task, learning the motor control and the conditions of reward and penalty, in a pretesting session that continued until performance approached a stable asymptote.
9. Electrodes were placed according to an expanded version of the standard 10-20 electrode system, in which additional coronal rows of electrodes were interposed between the original rows. The anterior midline parietal electrode was used as reference.
10. The band pass had a 6-decibel/octave roll-off below 0.1 Hz and a 24-decibel/octave roll-off above 50 Hz. The roll-off below 0.1 Hz was gradual enough to allow sensitivity to ultralow-frequency brain potential components.
11. B. Hjorth, *EEG Clin. Neurophysiol.* **39**, 526 (1975); *Am. J. EEG Technol.* **20**, 121 (1980); P. L. Nunez, *Electric Fields in the Brain: The Neurophysics of EEG* (Oxford Univ. Press, New York, 1981). This operation removed the effect of the reference channel. Peripheral channels were not transformed because application of the Laplacian operator to an electrode requires surrounding electrodes, which are absent for channels at the edge of a recording array. Sixteen channels remained: left and right frontal (F3 and F4); midline frontal (Fz); left and right antero-central (aC3 and aC4); midline antero-central (aCz); left and right central (C3 and C4); midline central (Cz); left and right antero-parietal (aP1 and aP2); midline antero-parietal (aPz); left and right parietal (P3 and P4); midline parietal (Pz); and midline antero-occipital (aOz).
12. For right- and left-hand accurate performance, mean error was 0.35 (range, 0.24 to 0.52) and 0.39 (range, 0.28 to 0.51), respectively. For right- and left-hand inaccurate performance, mean error was 1.62 (range, 1.18 to 1.96) and 1.66 (range, 1.40 to 2.18), respectively. Classifying performance separately for each individual compensated for between-subject performance differences; hence, each data set contained trials from each subject. Outlying trials on the distribution of recent performance level were eliminated to ensure that accurate and inaccurate data sets did not differ from each other according to factors that could be related to transitory changes in arousal. Accurate and inaccurate trials were evenly distributed throughout the recording session.
13. This approach is based on the hypothesis that when areas of the brain are functionally related, the wave shapes of their macropotentials are consistently similar [M. N. Livanov, *Spatial Organization of Cerebral Processes* (Wiley, New York, 1977); W. Freeman, *Mass Action in the Nervous System* (Academic Press, New York, 1975); in (*14*); A. Gevins *et al.*, *Psychophysiology* **22**, 32 (1985)].
14. A. Gevins and A. Remond, *Handbook of Electroencephalography and Clinical Neurophysiology* (Elsevier, New York, in press), vol. 1, chap. 8.
15. A. Gevins *et al.*, *Science* **213**, 918 (1981); A. Gevins *et al.*, *ibid.* **220**, 97 (1983).
16. Enhanced averages were formed from sets of trials selected as follows: for each channel, sets of single-trial data samples in a 250-msec interval centered 750 msec after the cue were submitted to a mathematical pattern classification program. The program attempted to discriminate the event-related trials from a "noise" data set with statistical properties similar to the ongoing electroencephalogram in corresponding channels. In each interval, significantly distinguished channels ($P < 0.05$) were tabulated for each person. The enhanced averages were formed from those trials in which a majority of the tabulated channels were significantly classified [A. Gevins, N. Morgan, S. Bressler, J. Doyle, B. Cutillo, *EEG Clin. Neurophysiol.* **64**, 177 (1986)].
17. The maximum absolute value of covariance was converted to a significance (after square-root transformation) by comparison with a noise median and an estimate of noise variance through the use of a Tukey biweight scale estimate. These statistics were determined from sample distributions of the square root of zero-lag covariances between intervals centered around samples with the minimum energy envelope derived from the Hilbert transform. Duncan's correction procedure was used to control for the 120 comparisons within each interval. Detailed signal-processing methods and analyses of stimulus-, response-, and feedback-related patterns have been developed (*18*).
18. A. Gevins *et al.*, in preparation.
19. D. H. Ingvar and L. Philipson, *Ann. Neurol.* **2**, 230 (1977); C. F. Pieper, S. Goldring, A. B. Jenny, J. P. McMahon, *EEG Clin. Neurophysiol.* **48**, 266 (1980); A. Foit, B. Larsen, S. Hattori, E. Skinhoj, N. A. Lassen, *ibid.* **50**, 426 (1980); P. E. Roland, B. Larsen, N. A. Lassen, E. Skinhoj, *J. Neurophysiol.* **43**, 118 (1980). The major peak in the Laplacian waveform during the response was centered 62 msec after response onset and was approximately 190 msec wide; therefore, a 4- to 7-Hz bandpass filter and a covariance interval of 187 msec were used. Given the high signal strength of overt movement and the resulting large number of significant response-related covariances, only the top standard deviation of significant covariances could be shown in Fig. 1 without creating an overly complex display. If all significant covariances are considered, left-sided covariances were significantly greater than the comparable right-sided ones by the [$t(78) = 18.5$, $P < 0.0001$] for the right-hand response. Significant right-sided covariances were significantly greater than the left-sided ones [$t(78) = 21.5$, $P < 0.001$] for the left-hand response. The right antero-central electrode site did not appear in the left-hand pattern in Fig. 1 because its significance was slightly below the 1-SD cutoff.
20. We made amplitude maps by determining the average amplitude of the Laplacian waveform for each electrode site over the same interval used to calculate covariances and interpolating between sites. Amplitude was represented on a color scale, with red representing the maximum and violet the minimum.
21. A delta filter (low-pass cutoff at 3 Hz) and a covariance interval width of 375 msec were used to study the low-frequency CNV component.
22. Comparison by the t test of mean-squared amplitude, measured on each Laplacian waveform (over the same 500- to 875-msec-centered postcue interval as was used for the between-channel covariance) between subsequently accurate and inaccurate conditions of each hand, was not significant at $P < 0.05$. Similarity between the sets of CNV amplitudes, or the two covariance maps, was measured with an estimate of the correlation and its confidence interval. (Correlation was not used in this context to assess linear dependence.) For the small number of repeated measures, a normal distribution could not be confirmed. Therefore, robust, resistant estimates were calculated with a distribution-independent "bootstrap" Monte Carlo procedure [B. Efron, *The Jacknife, The Bootstrap, and Other Resampling Plans* (Society for Industrial and Applied Mathematics, Philadelphia, 1982)], which generates an ensemble of correlation values from randomly selected choices of the repeated measures. When the distributions of CNV amplitudes from subsequently accurate and inaccurate conditions were compared according to this procedure, the correlations were 0.84 ± 0.16 before right-hand performance and 0.83 ± 0.14 before left-hand performance. Thus, it is not possible to discriminate between subsequently accurate and inaccurate waveforms on the basis of the mean-squared amplitude of the averaged event-related CNV waveforms.
23. These four sites were the most prominent in that the numbers of significant covariances in which they were involved each exceeded half of the maximum number of any site (nine for the antero-parietal site). The other sites in the pattern were involved in one-third or fewer of that maximum. The same criterion was used to judge which sites were most prominent in the left-hand pattern.
24. In addition to the cue-to-stimulus period, the post-stimulus and postfeedback periods also differed in accuracy, but the response period did not (*18*). The signal strength of prestimulus covariances was much smaller than those during overt responses, that is, the scale of significance was three orders of magnitude smaller. The smaller number of prestimulus covariances allowed all significant covariances to be shown in Fig. 4. Comparison by t test of the sets of subsequently accurate and inaccurate covariances was significant at $P < 0.001$ for both left- [$t(38) = 5.57$] and right-hand [$t(23) = 7.70$] comparisons. The bootstrap correlation (*22*) between covariance patterns before subsequently accurate and inaccurate performance from channel pairs that were significant for either condition was 0.57 ± 0.09 for the right hand and 0.10 ± 0.14 for the left hand. The t test and bootstrap correlation results, taken together, suggest that the left-hand accurate and inaccurate conditions differ both in scale and in pattern, whereas right-hand results differ only in scale.
25. The classifier was a nonlinear, two-layered, adaptive decision network [(*15*); A. Gevins *et al.*, *Science* **203**, 665 (1979); A. Gevins *et al.*, *Psychophysiology* **22**, 32 (1985)] that decided whether subsequent performance was accurate or inaccurate from CNV-interval, between-channel covariances of each trial. This algorithm produced, by a recursive procedure, classification equations consisting of weighted combinations of the decisions of discriminant functions, which themselves consisted of weighted combinations of a subset of the covariance values of Fig. 4. Cross-validation of the equations was performed by testing equations on data that were not used to derive them. Significance was determined according to the binomial distribution. Details of the application of pattern classification procedures to the analysis of brain signals have been presented [A. Gevins, *IEEE Trans. Pattern Anal. Mach. Intell.* **2**, 282 (1980); in (*14*), chap. 17; ——— and N. Morgan, *IEEE Trans. Biomed. Eng.*, in press]. These conservative procedures notwithstanding, we must caution that the degree of generalization of these results to the population at large is unknown and can be determined only by additional studies with new subjects.
26. Previous studies that measured interelectrode correlation have suggested a cortical origin for these patterns (*13–15*). The difficult problem of identifying the generators of these patterns is the focus of current work. At present, the focal, spatially separated patterns tend to rule out volume-conducted activity from one or two cortical or subcortical generators.
27. D. Ruchkin, S. Sutton, D. Mahaffey, *EEG Clin. Neurophysiol.* **63**, 445 (1986).
28. V. B. Mountcastle, *J. R. Soc. Med.* **71**, 14 (1978); B. Lee, H. Luders, R. Lesser, D. Dinner, H. Morris, *Ann. Neurol.* **20**, 32 (1986).
29. G. Goldberg, *Behav. Brain Sci.* **8**, 567 (1985).
30. Supported in part by grants and contracts from the Air Force Office of Scientific Research, the Air Force School of Aerospace Medicine, the National

Science Foundation, and the National Institutes of Neurological and Communicative Disorders and Strokes, National Institutes of Health. We thank G. Zeitlin, R. Tannehill, and B. Costales for programming, J. Salzman for data analysis, K. Dean and J. Toal for manuscript preparation, and D. F. Benson, J. Halliday, M. Kutas, R. Parasuraman, C. Rebert, W. Ritter, and J. Rohrbaugh for comments on earlier versions of this manuscript. This report is dedicated to the memory of Samuel Sutton for his seminal contributions to the study of human psychophysiology.

20 May 1986; accepted 10 October 1986

Diurnal Expression of Transducin mRNA and Translocation of Transducin in Rods of Rat Retina

MARK R. BRANN* AND LESLIE V. COHEN

The messenger RNA (mRNA) that encodes α subunit of the guanosine triphosphate–binding protein transducin (T_α) and T_α immunoreactivity were localized and measured in the rat retina during the light-dark cycle with in situ hybridization and immunohistochemistry. Both T_α mRNA and T_α immunoreactivity were observed only in photoreceptors. Within the photoreceptor T_α mRNA was present primarily in the inner segments and to a lesser extent in the outer nuclear layer at all times during the day and night. However, the distribution of T_α immunoreactivity varied profoundly with the light-dark cycle; during the day, T_α immunoreactivity was highest in the inner segments, and at night the outer segments were more immunoreactive. The amounts of T_α mRNA and T_α immunoreactivity also depended on the light-dark cycle. Levels of T_α mRNA were high immediately before and after lights on; levels were low for the rest of the light-dark cycle. During the day, T_α immunoreactivity increased in the inner segments following the increase in T_α mRNA. After the lights were turned off, T_α immunoreactivity decreased in the inner segments and increased in the outer segments. Thus, it appears that T_α is synthesized in the inner segments after a morning increase in T_α mRNA. Newly synthesized T_α remains in the inner segments until it is transported to the outer segments at night, where it may be involved in the increase in the sensitivity of photoreceptor rods at night.

TRANSDUCIN IS A GUANOSINE TRIphosphate (GTP)–binding (G) protein that mediates the stimulation of guanosine 3′,5′-monophosphate phosphodiesterase by light-activated rhodopsin in photoreceptor rods. Transducin is a membrane-associated protein that consists of three subunits—α, β, and γ. The α subunit (T_α) is structurally and functionally homologous to the α subunits of the G proteins that mediate inhibition of adenylate cyclase by neurotransmitter receptors. The β subunit of transducin may be identical to the β subunit of the G proteins that are associated with adenylate cyclase (*1*). Although the structure of transducin and the molecular characteristics of its coupling with rhodopsin have been extensively investigated, little information is available concerning either the regulation of the synthesis or the subcellular distribution of transducin by changes in physiological states. We localized and measured the expression of T_α messenger RNA (mRNA) and the subcellular distribution of T_α in photoreceptors during the light-dark cycle. T_α immunoreactivity was measured with immunohistochemistry and T_α mRNA was measured with in situ hybridization histochemistry.

Male Sprague-Dawley rats were maintained under a 12-hour light-dark cycle for 4 weeks before the localization studies were performed. Four animals were sacrificed every 4 hours during the light-dark cycle (under dim red light during the night); eyes were immediately removed, frozen on powdered dry ice, and stored at −80°C until 12-μm frozen sections could be prepared and mounted on gelatin-coated slides. Before the histochemical procedures, the slide-mounted tissue sections were thawed and kept at room temperature for 10 minutes, then fixed in 4% formaldehyde for 20 minutes. Immunohistochemical localization of T_α was performed with the peroxidase antiperoxidase (PAP) method (*2*) with a highly selective polyclonal antibody against T_α (*3*). The PAP reaction product was measured in photoreceptor inner and outer segments (*4*) and T_α mRNA was localized and measured (*5*). The synthetic oligodeoxynucleotide probe, complementary to nucleotides 1070 to 1117 of bovine T_α (*6*), was made by solid-phase synthesis on an Applied Biosystems DNA synthesizer and labeled with terminal deoxynucleotidyl transferase (BRL) and [^{35}S]deoxyadenosine triphosphate (NEN). Retinal sections were incubated with the complementary DNA (cDNA) probe at 37°C for 24 hours and washed under conditions of high stringency (18°C below the theoretical melting temperature). The distribution of labeled mRNA was evaluated by autoradiography (*5, 7*).

The specificity of our cDNA-T_α mRNA hybridization procedures was verified (*7*) by meeting four criteria: (i) Only cells within the photoreceptor cell layer were positive for T_α immunoreactivity and T_α mRNA; in the rat retina this cell layer almost exclusively contains photoreceptor rods. (ii) Hybridizations were performed under conditions of high stringency that precluded cross-hybridization even with mRNA's for related G proteins. (iii) A negative control for sequence-independent hybridization was established with a synthetic probe for tyrosine hydroxylase mRNA, which is not expressed within photoreceptors. (iv) A single band on a Northern blot of total RNA was observed with our cDNA probe at a hybridization stringency identical to that used for in situ hybridization.

T_α mRNA was only present in photoreceptors, was more abundant in the inner segments than the outer nuclear layer, and was absent from the outer segments (Fig. 1A). Qualitatively this distribution of T_α mRNA was the same at all times of day and night. On the other hand, the distribution of T_α immunoreactivity was distinctly different at night than during the day. During the day, T_α immunoreactivity was most pronounced in the inner segments, was less evident in the outer nuclear and plexiform layers, and was low in the outer segments (Fig. 1B). At night, T_α immunoreactivity was most dense in the outer segments, relatively little was present in the inner segments, and none was observed in the outer nuclear and plexiform layers (Fig. 1C). The only cells other than photoreceptors observed to have T_α immunoreactivity were in the pigment epithelium where immunoreactivity was most dense at 3:00 a.m. and 7:00 a.m., the time of peak disk shedding. Because these cells phagocytose the disks shed from the distal end of photoreceptors, this localization of T_α immunoreactivity in the pigment epithelium indicates that some T_α is shed with the photoreceptor disks.

T_α mRNA levels varied with the light-dark cycle (Fig. 2B). At night, levels of T_α mRNA were low, but they increased just prior to the onset of light. In the morning, T_α mRNA was at its highest level. By mid-

Laboratory of Cell Biology, National Institute of Mental Health, Room 3A-17, Building 36, Bethesda, MD 20892.

*Present address: Metabolic Diseases Branch, National Institute of Diabetes and Digestive and Kidney Diseases, Room 9C-101, Building 10, Bethesda, MD 20892.